

## Grafting of alginates on UF/NF ceramic membranes for wastewater treatment

C.P. Athanasekou<sup>a</sup>, G.E. Romanos<sup>a,\*</sup>, K. Kordatos<sup>b</sup>, V. Kasselouri-Rigopoulou<sup>b</sup>, N.K. Kakizis<sup>a</sup>, A.A. Sapalidis<sup>a</sup>

<sup>a</sup> Institute of Physical Chemistry, NCSR Demokritos, 15310 Agia Paraskevi, Attikis, Greece

<sup>b</sup> School of Chemical Engineering, National Technical University of Athens, 9 Heroon Polytechniou Street, 15780 Zografou, Greece

### ARTICLE INFO

#### Article history:

Received 24 December 2009

Received in revised form 17 June 2010

Accepted 18 June 2010

Available online 25 June 2010

#### Keywords:

UF/NF membranes

Grafting

Alginates

Metal retention

Acidic regeneration

Silanes

### ABSTRACT

The mechanism of heavy metal ion removal in processes involving multi-layered tubular ultrafiltration and nanofiltration (UF/NF) membranes was investigated by conducting retention experiments in both flow-through and cross-flow modes. The prospect of the regeneration of the membranes through an acidic process was also examined and discussed. The UF/NF membranes were functionalised with alginates to develop hybrid inorganic/organic materials for continuous, single pass, wastewater treatment applications. The challenge laid in the induction of additional metal adsorption and improved regeneration capacity. This was accomplished by stabilizing alginates either into the pores or on the top-separating layer of the membrane. The preservation of efficient water fluxes at moderate trans-membrane pressures introduced an additional parameter that was pursued in parallel to the membrane modification process. The deposition and stabilization of alginates was carried out via physical (filtration/cross-linking) and chemical (grafting) procedures. The materials developed by means of the filtration process exhibited a 25–60% enhancement of their Cd<sup>2+</sup> binding capacity, depending on the amount of the filtered alginate solution. The grafting process led to the development of alginate layers with adequate stability under acidic regeneration conditions and metal retention enhancement of 25–180%, depending on the silane involved as grafting agent and the solvent of silanisation.

© 2010 Elsevier B.V. All rights reserved.

### 1. Introduction

Extraction techniques for the removal of heavy metals from wastewater streams have lately gained significant research attention. Cadmium released from a wide range of natural and anthropogenic sources is one of the main toxic inorganic pollutants. It accumulates in living tissues through the food chain, influencing all living organisms and mostly human beings [1,2]. This element can be removed from wastewater by conventional processes such as chemical precipitation/filtration, ion exchange and adsorption or according to latest developments by pressure-driven membrane processing. As growing attention has been attracted to the potential health hazard arising from the existence of heavy metals in the environment, the need for cost effective and efficient methods for the removal of metals has resulted in the development of new separation technologies. Precipitation, adsorption-ion exchange, flocculation, absorption, electrochemical processes and/or membrane processes such as electrodialysis, nanofiltration and reverse

osmosis, are commonly applied for the treatment of industrial effluents [3–6]. In a previous work we introduced [7] a novel method of functionalisation of inorganic membranes with alginate, which is a low cost biopolymer with enhanced heavy metal adsorption capacity [8]. The developed hybrid membranes allowed for heavy metal ions removal from wastewater at low pressure(s) and high throughput rates. An advantage of membrane-based sorbents is that functional groups can be attached to the membrane pores as polymeric ligands, rather than as monomeric surface functional groups. By means of interposing the functional groups along the flow path where contaminated solutions are channeled through the porous structure, the resulting interaction between functional groups and heavy metal ions is significantly amplified. As a result accessibility and solute contact is enhanced, resulting in better overall material performance. Under the framework of the current study, the challenge was to stabilise the biopolymer on the membrane surface through covalent bonding, without further applying a metal induced cross-linking procedure that would consume a large portion of the polymer's binding groups (–COOH). The chemical process treatment developed, consisted of acidic hydrolysis/rehydroxylation and silanisation of the membrane's separating layer with 3-glycidyloxypropyltrimethoxysilane (GPTS), followed by epoxy ring opening and reaction with the car-

\* Corresponding author at: Institute of Physical Chemistry, NCSR Demokritos, Terma Patriarchoy Grigoriy & Nea, Athens, Greece. Tel.: +30 2106503972.

E-mail address: [groman@chem.demokritos.gr](mailto:groman@chem.demokritos.gr) (G.E. Romanos).

boxyl/hydroxyl groups of the alginates. An alternative chemical modification route consisted of rehydroxylation and silanisation with chlorotrimethoxy silane, followed by methoxy group hydrolysis and bonding with the alginate hydroxyls. In numerous occasions, the grafting procedure by means of GPTS has been described in the literature as a way for the preparation of size exclusion columns that are applied in HPLC chromatography [9–13]. In the current work, the procedure was evaluated as a means of stabilizing a metal adsorbing biopolymer on the surface of ceramic UF/NF membranes.

The metal efficiency of the “chemically” prepared membranes was selected as a primary indicator and was compared to the respective values exhibited by membranes modified by an alternative “physical” process. The physical process in question, involved filtration of sodium alginate solutions through the membrane’s pores, followed by cross-linking of the entrapped alginates with  $\text{Ca}^{2+}$ .

The grafting process resulted in hybrid membranes that exhibited enhanced metal binding capacity, combined with satisfactory overall material stability. These properties render the developed materials as excellent candidates for continuous single pass wastewater treatment applications.

## 2. Experimental

### 2.1. Materials

Tubular nanofiltration and ultrafiltration membranes (tubes of 15 cm length, 0.7 cm ID, 1 cm OD, glazed ends 1.5 cm) with active NF/UF area of a 26 cm<sup>2</sup> were obtained from Inopor<sup>®</sup>. The tubes consisted of a macroporous  $\alpha$ -alumina support (2.5  $\mu\text{m}$  mean pore size), two intermediate  $\gamma$ -alumina layers of mean pore size 1.0  $\mu\text{m}$  and 0.2  $\mu\text{m}$  respectively and a top-separating layer of 1.5  $\mu\text{m}$  thickness, located on the inner side of the tubes. The pore size for the UF  $\gamma$ -alumina layers was 5 nm and 10 nm and for the NF silica layer 1 nm. All the other necessary chemicals used in the study were of analytical grade and were applied without further purification. Weighed quantities of  $3\text{CdSO}_4 \cdot 8\text{H}_2\text{O}$  (Merck), sodium alginate derived from *Macrocystis pyrifera* (Sigma A-2158), calcium chloride (Sigma) and sodium hydroxide (Sigma) were dissolved in ultra pure water (Easy RO Barnstead). 3-Chloropropyl-trimethoxysilane (Sigma) and 3-glycidoxypropyltrimethoxysilane >98% (Sigma) was dissolved in chloroform (Lab-Scan), toluene, acetonitrile, and methanol (Fluka). Hydrogen peroxide 30% (w/v) (Panreac), sulfuric and nitric acid 65% (Redel-de-Haën) were also used. For the surface titrations glacial acetic acid 70%, chloroform, starch tetraethylammonium bromide reagent (Merck), sodium hydrogencarbonate, perchloric acid (Riedel-de-Haën), sodium arsenite (Carlo Erba), periodic acid and Fixanal I<sub>2</sub> 0.005 mol ampoule (Sigma) were used.

### 2.2. Analytical methods

The total organic carbon content (TOC) in the water samples was determined with a Dohrman DC80 “total carbon analyser”. The measurements were based on the UV promoted potassium persulfate oxidation method. The instrument was calibrated with potassium hydrogen sulfate solutions (KHP) in the 0–200 ppm and 0–2000 ppm ranges and the injection volume was 200  $\mu\text{L}$  and 40  $\mu\text{L}$ , respectively.

The carbon content of the solid samples was determined with an ELTRA CS-800 analyser equipped with a high frequency induction furnace, two IR cells for carbon and one for sulfur. About 200 mg of the sample were mixed with 2 g of tungsten and 0.7 g of iron to ensure proper heating of the ceramic sample and combustion with oxygen.

The  $\text{Cd}^{2+}$  content of the water was determined by AAS spectroscopy (GBC Avanta).

SEM images were obtained with a JEOL (JSM-7401F) Field Emission electronic microscope equipped with EDS.

The water adsorption experiments were performed with a gravimetric analyzer (IGA-100) supplied by Hiden Isochema Ltd. Before each measurement, a sample mass of about 300 mg was outgassed at high vacuum ( $10^{-5}$  mbar) and a temperature of 160 °C.

The population of surface anchored oxirane groups was determined by the direct titration with standard perchloric acid in acetic acid and in the presence of an excess of a soluble quaternary ammonium bromide, to the crystal violet end-point [14]. The vicinal diols (opened epoxide groups) population was determined by the periodate oxidation method, followed by iodine back titration [9]. A portion of 2–3 g of the functionalised membrane in the form of a powder was involved in all titration experiments.

### 2.3. Membrane functionalisation

The procedure for the filtration/cross-linking of the alginates was attempted in both the flow-through (FT) and cross-flow (CF) modes (Fig. 1), by filtering the solutes from the macroporous support and the separation layer of the membrane tube, respectively. For the silanisation/alginate-bonding, the CF technique was applied and the reactants were introduced from the inner separation layer of the membrane.

In the case of alginates filtration/cross-linking, 10 nm and 5 nm  $\gamma$ -alumina ultrafiltration and 1 nm silica nanofiltration membranes were involved, with respective MW cut-off thresholds of 50, 7.5 and 0.6 kDa. An alginic acid solution of 1.5% (w/w) (MW 76 kDa) was used for filtration. To this effect, deposition was confined just into the larger pores of the membrane support. As illustrated in Fig. 1a, a constant flow stream (0.5–10 ml/min, depending on the membrane pore size) of the alginic acid solution was continuously fed to the annular space of the reactor via a fluid accumulator A equipped with a floating piston driven by a high precision HPLC pump B (Waters 515 series) that delivered deionised water as the confining liquid D in the downstream space of the fluid accumulator. Under these constant flow conditions, extreme reduction of the permeability factor due to deposition of alginates was avoided by continuously monitoring the fluid pressure in the reactor cell by means of the electronic pressure transducer of the HPLC pump. By applying the alginates mass balance equation between the feed and permeate F side of the membrane, it was possible to calculate the total amount of retained alginates. The alginates content of the aliquots, collected from the exhaust stream F of the reactor during deposition, was determined by organic carbon (TOC) analysis. A similar procedure was followed for the subsequent cross-linking procedure with the  $\text{Ca}^{2+}$  solution in order to define the portion of alginates leached away and calculate their net amount stabilised into the pores.

For the silanisation/alginate-bonding modification, 5 nm and 10 nm  $\gamma$ -alumina ultrafiltration membranes were involved, which were previously activated under the optimum conditions described in Section 3.2. The silanisation took place on the separating layer of the membrane in the cross-flow mode (Fig. 1b) by switching the position of the three way valves V1, V2, V3. A backpressure regulator C (TESCOM EUROPE, 26-1762-24-090) controlled the pressure of the fluid in the inner space of the membrane tube. Under these constant pressure conditions, extreme reduction of the permeability factor due to silane grafting was avoided by continuously monitoring the proportion of effluent volumes gathered from the retentate E and permeate K side of the membrane.

The silanisation reaction temperature was 80 °C and was maintained by means of a PID temperature controller and a heating tape G wrapped around the reactor cell. In the case of utilizing

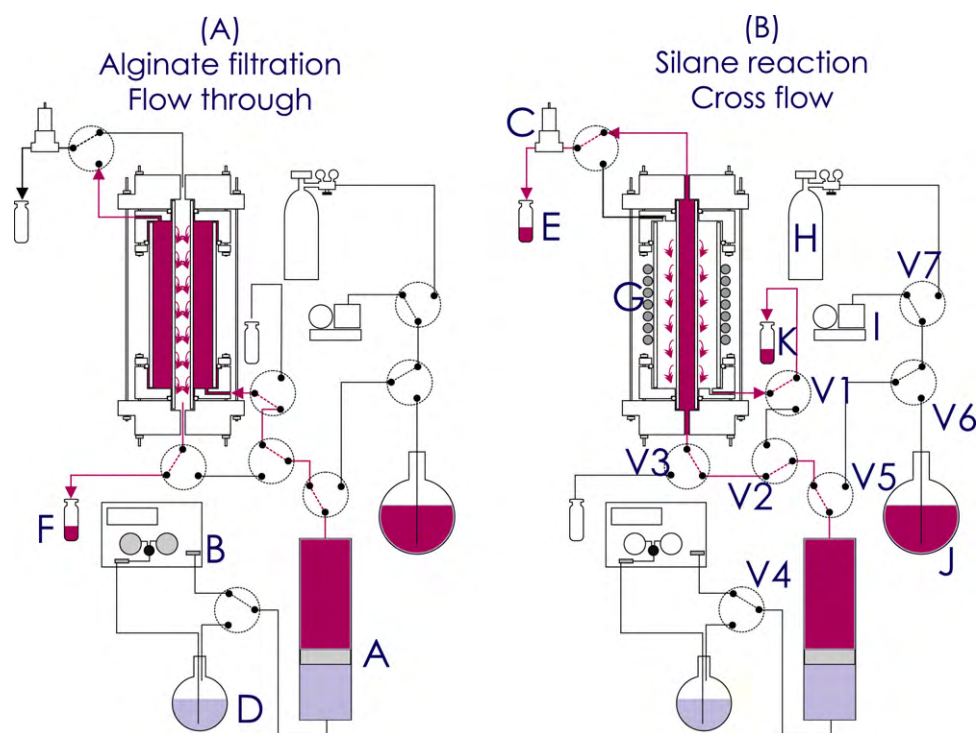


**Fig. 1.** Device constructed for membrane functionalisation and performance evaluation: (a) alginate filtration & flow-through experiments and (b) silane reaction & cross-flow experiments.

chloroform as the silane solvent, the fluid accumulator, tubing and internal space of the membrane were sequentially washed with toluene, acetonitrile, methanol and water before proceeding with the subsequent reaction with alginates. The three way valves V4–V7 served the following actions: (1) drawing down the piston in the fluid accumulator via gas pressure provided from a cylinder containing argon H, (2) evacuating the upstream space of the fluid accumulator via the rotary pump I and (3) refilling the fluid accumulator from the reactant solution flask J under vacuum.

Table 1 presents the coding scheme used for the identification of every sample. Each sample was identified with respect to the treatment conditions used and the results obtained through the implementation of the applied analytical techniques.

#### 2.4. Membrane performance

The metal retention efficiency was examined in the apparatus used for the functionalisation (Fig. 1) and without the need to dismantle the membrane. It is important to note that the terms CF and FT, included in the materials sample coding presented in Table 1, solely define the modification procedure and has no implications with respect to the metal retention efficiency measurement. All the metal retention experiments were carried-out by feeding the  $\text{Cd}^{2+}$  solution from the inner separating layer side of the membrane tube. After the final alginate filtration (or reaction) phase and before proceeding to performance related experiments, the fluid accumulator and tubing up to the valves V1 and V3 (Fig. 1) were properly washed with plenty of deionised water. In addition,

**Table 1**  
Carbon content (theoretical and experimental) of all samples.

Sample code	–OH (mmol/g) derived from water isotherm	C% predicted from –OH population	Elemental analysis, C%
Al/5/w	0.022	–	–
Al/5/m	0.11	–	–
Al/5/s	0.19	–	–
Al/5	0.03	–	–
Al/5/C6/HC	0.03	0.18	0.14
Al/5/w/C6/HC	0.022	0.13	0.09
Al/5/m/C6/HC	0.11	0.63	0.15
Al/5/s/C6/HC	0.19	1.1	0.17
Al/5/w/C6/HC/alg/FT	0.022	NA	0.073
Al/5/C6/HC/alg/FT	0.03	NA	0.107
Al/5/s/C6/HC/alg/FT	0.19	NA	0.29
Al/5/m/C6/HC/alg/FT	0.11	NA	0.212
Al/5/C9/HC	0.03	0.29	0.12
Al/5/s/C9/OH7/CF	0.19	1.83	0.32
Al/5/s/C9/OH7/alg/CF	0.19	NA	0.56
Al/5/s/C9/OH8.5/CF	0.19	1.83	0.9

The sample code consists of seven parts with reference to: layer material/layer pore size (nm)/way of activation: s, strong ( $1/4 \text{H}_2\text{O}_2/\text{H}_2\text{SO}_4$ ); m, moderate ( $2/3 \text{H}_2\text{O}_2/\text{H}_2\text{SO}_4$ ); w, weak ( $\text{H}_2\text{O}_2$ )/silane type: C9,  $\text{C}_9\text{H}_{20}\text{O}_5\text{Si}$ ; C6,  $\text{C}_6\text{H}_{15}\text{O}_3\text{SiCl}$ /silane solvent: HC,  $\text{CHCl}_3$ ; OH7,  $\text{H}_2\text{O}$ -pH = 7; OH8.5,  $\text{H}_2\text{O}$ -pH = 8.5/alg = treatment with alginates/mode of treatment (FT, flow-through; CF, cross-flow).

**Table 2**  
Operating characteristics of the examined unmodified membranes.

	Pore size (nm)	PZC	Volume flux ( $\times 10^6$ m <sup>3</sup> /m <sup>2</sup> /s)	Pressure (MPa)	Perm. ( $\times 10^{20}$ m <sup>2</sup> )	Mode
Si/1/FT	1	3	58	10	0.58	Flow-through
Al/10/FT	10	8.5	64.1	0.023	28	Flow-through
Si/1/CF	1	3	4.98	4.5	0.1	Cross-flow
Al/5/CF	5	8.5	13.5	3.88	0.35	Cross-flow
Al/10/CF	10	8.5	26.3	5.2	0.51	Cross-flow

several milliliters of pure deionised water were allowed to wash the internal and external area of the membrane tube in the cross-flow mode. The effluents were collected and analysed for their carbon content in order to obtain a first indication on the stability of the deposited or reacted alginates and calculate their net mass on the membrane at the beginning of each metal retention experiment.

Before proceeding with the evaluation of the hybrid inorganic/alginate membranes, it was necessary to perform Cd<sup>2+</sup> retention/regeneration experiments on the involved UF/NF supports. In this way it was possible to elucidate the extent of improvements brought about as a result of the functionalisation and study the possible mechanisms of heavy metal exclusion on two different metal-oxide surfaces, like alumina and silica, with different opposite electrical charge at the applied solute concentration/pH and different pore size ranging from nanofiltration ( $d_p < 2$  nm) to ultrafiltration ( $100 > d_p > 2$ ).

An aquatic solution of 3CdSO<sub>4</sub>·8H<sub>2</sub>O with a concentration of 100 ppm Cd<sup>2+</sup> and pH = 4.8 was involved in all the experiments that were performed in both the CF and FT modes for the unmodified

samples and in the CF mode for the hybrid samples. In Table 2, the characteristics of the examined unmodified membranes together with the values of some experimental parameters during performance evaluation are presented.

### 3. Results and discussion

#### 3.1. SEM-EDS analysis

Fig. 2a is a SEM image of the cross-section of the untreated membrane (Al5) showing its asymmetric structure that consists of a rough  $\alpha$ -alumina support, two intermediate macroporous  $\gamma$ -alumina layers and an ultra-thin nanofiltration  $\gamma$ -alumina layer. In Fig. 2b we present the cross-section of the second intermediate  $\gamma$ -alumina layer (immediately below the nanofiltration layer) with a pore size of 0.25  $\mu$ m. Fig. 2c and d presents in comparison the surface morphology of the  $\gamma$ -alumina nanofiltration layer (5 nm) before and after the silanisation/reaction procedure. As it is clear the grafted alginates altered the microstructure of the  $\gamma$ -alumina

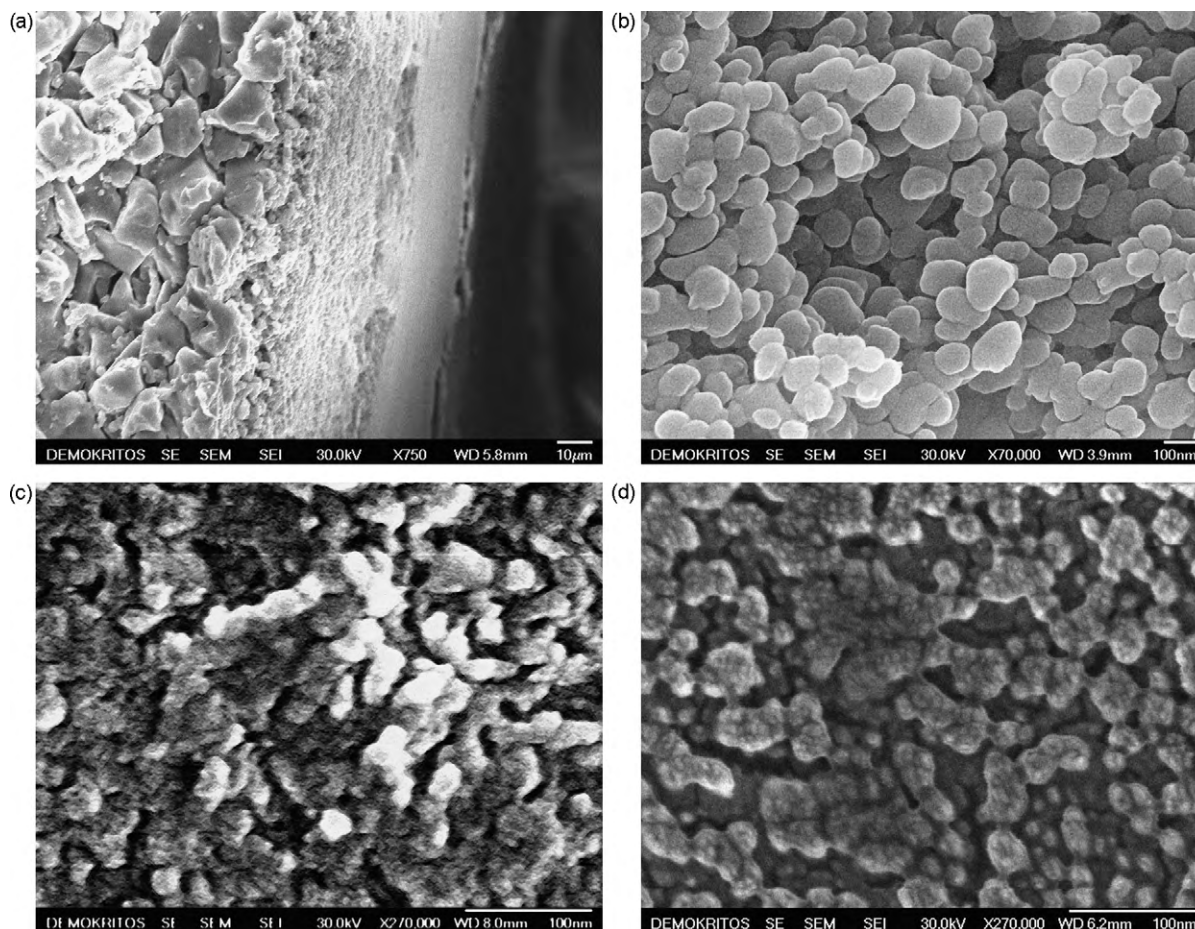


**Fig. 2.** SEM images of (a) the cross-section of the unmodified  $\gamma$ -alumina 5 nm membrane, (b) the intermediate  $\gamma$ -alumina layer with pores of 0.2  $\mu$ m, (c) the NF layer of the unmodified  $\gamma$ -alumina 5 nm membrane and (d) the NF layer of the  $\gamma$ -alumina 5 nm membrane after silanisation and reaction with alginates.

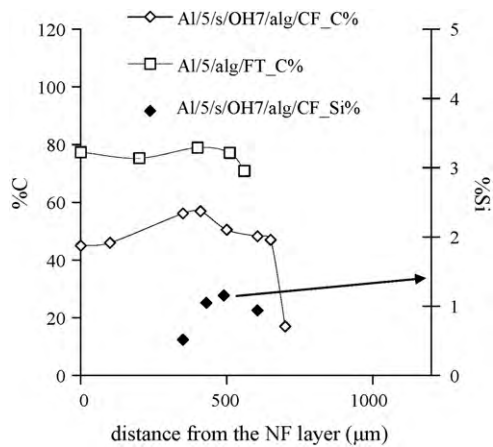


Fig. 3. EDS analysis of the vertical cross-section of membranes derived by the alginates filtration and the silanisation/alginate reaction procedures.

layer which became smoother and denser and the borders between the alumina nanoparticles are hardly distinguished.

In Fig. 3 we present the results of EDS analysis along the vertical cross-section of the membrane tube as a function of the distance from the NF layer.

Silicon (Si) was detected at a depth of about 600 μm, for membrane Al/5/s/OH7/alg/CF, revealing that the silanisation reaction was not confined just in the area of the nanofiltration layer, but also occurred into the subsequent macroporous layers. The carbon content of the membrane derived from the alginates filtration/cross-linking procedure (Al/5/alg/FT) is higher than that of the membrane produced by means of the silanisation/alginate reaction process (Al/5/s/OH7/alg/CF). This however holds immediately after the development of the two membranes. As will be shown in Section 3.3.3 the silanised membrane exhibited enhanced stability and it retained a much higher amount of alginates after its subjection to repeating cycles of metal retention/acid regeneration processes.

### 3.2. Alumina surface activation—silanisation—surface titration

The surface activation (rehydroxylation) of the separating layer was performed by treating the membrane for half an hour in boiling acidic solutions of the following composition: (A) 30% H<sub>2</sub>O<sub>2</sub> (w = weak), (B) 2/3 (v/v) H<sub>2</sub>O<sub>2</sub>/H<sub>2</sub>SO<sub>4</sub> (m = moderate) and (C) 1/4 (v/v) H<sub>2</sub>O<sub>2</sub>/H<sub>2</sub>SO<sub>4</sub> (s = strong).

The efficiency of the aforementioned treatments was evaluated via gravimetric water vapor adsorption experiments at 35 °C and calculation of the BET monolayer capacity. The results obtained are depicted in Fig. 4. It should be noted that before each measurement, the g-alumina separating layer was mechanically removed from the membrane surface and smashed in a mortar to form a powder that was further subjected to outgassing at elevated temperatures and high vacuum (10<sup>-5</sup> mbar).

The optimum outgassing temperature was 160 °C since this value is often referred [15,16] as a threshold for not affecting the population of surface hydroxyls through condensation reactions. In this manner, it was possible to derive the -OH group's concentration in mmol/g by assuming a one per one interaction of the surface hydroxyl groups with the water molecules. The results have been already presented in Table 1 along with the predicted carbon content after silanisation and the carbon content C% defined following the elemental analysis carried out after silanisation and after silanisation and subsequent reaction with the alginates respectively. The predicted C% values were derived by assuming that each silane molecule is anchored to one hydroxyl of the solid surface through

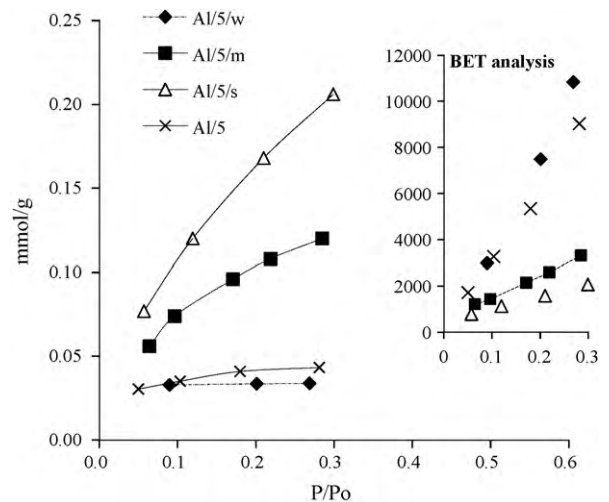


Fig. 4. Water vapor adsorption curves of the activated samples (inset: BET analysis).

one of its alkoxy groups with a type II SN<sub>2</sub> reaction mechanism. The choice of chloroform was intentional and was based on the fact that chloroform, a polar solvent, was expected to enhance reactivity for the envisaged reaction mechanism where the reactants are neutral.

As it can be observed (Fig. 4), optimum enhancement of the hydroxyl groups' concentration was achieved for the sample Al/5/s, which was treated with the more acidic solution (1/4 H<sub>2</sub>O<sub>2</sub>/H<sub>2</sub>SO<sub>4</sub>).

In the case of the silanised samples with low hydroxyl content like the samples Al/5/C6/HC and Al/5/w/C6/HC, the predicted C% content after silanisation comes into convergence with the outcome of elemental analysis (Table 1) indicating the substantiality of the hypothesis that the chlorosilanes were attached to the surface with only one of their alkoxy groups. In the cases of higher hydroxyl content, as it is for samples Al/5/m/C6/HC and Al/5/s/C6/HC, the closeness of the more densely located hydroxyls allows for anchoring of each silane molecule with more than one alkoxy groups and this explains the sufficiently lower experimentally derived C% values compared to the predicted ones. It is also important to note that for the chlorosilane samples with low starting content of hydroxyl groups (Al/5/C6/HC, Al/5/w/C6/HC) there was no retention of amount of alginates during the treatment with the aquatic solution of sodium alginate (see Table 1 samples Al/5/w/C6/HC/alg/FT and Al/5/C6/HC/alg/FT). A possible explanation is that in the case of low silane coverage, the subsequent contact with the aquatic solution hydrolyses the unreacted alkoxy groups and thus, the adjacent grafted silanes are polymerised on the alumina surface as illustrated in Fig. 5a. Thereby, all the alkoxy groups that are converted into hydroxyl are consumed through silane polymerisation and there is no binding group for the oncoming alginic acid molecules. On the other hand, elemental analysis resulted in higher carbon content after the reaction with alginates (Table 1, Al/5/s/C6/HC/alg/FT, Al/5/m/C6/HC/alg/FT) for the samples characterised by high initial population of surface hydroxyls. In this case, silanes consume all or two of their alkoxy groups for their anchoring with the solid surface. Thus, there exists the possibility of a silanised surface configuration, like the one presented in Fig. 5b, where adjacent silanes still retain one of their alkoxy groups but there is no neighbouring group for polymerisation to be initiated during hydrolysis caused by contact with the aquatic alginic acid solution. In this way, the oncoming alginates (polysaccharides) are covalently bonded through their hydroxyl groups to the silanols generated due to hydrolysis, as illustrated in Fig. 5b.

In the case of the 3-glycidoxypropyltrimethoxysilane (GPTMS), the situation is more complicated due to the high reactivity of the oxirane ring. The surface-bonding reactions can take place through

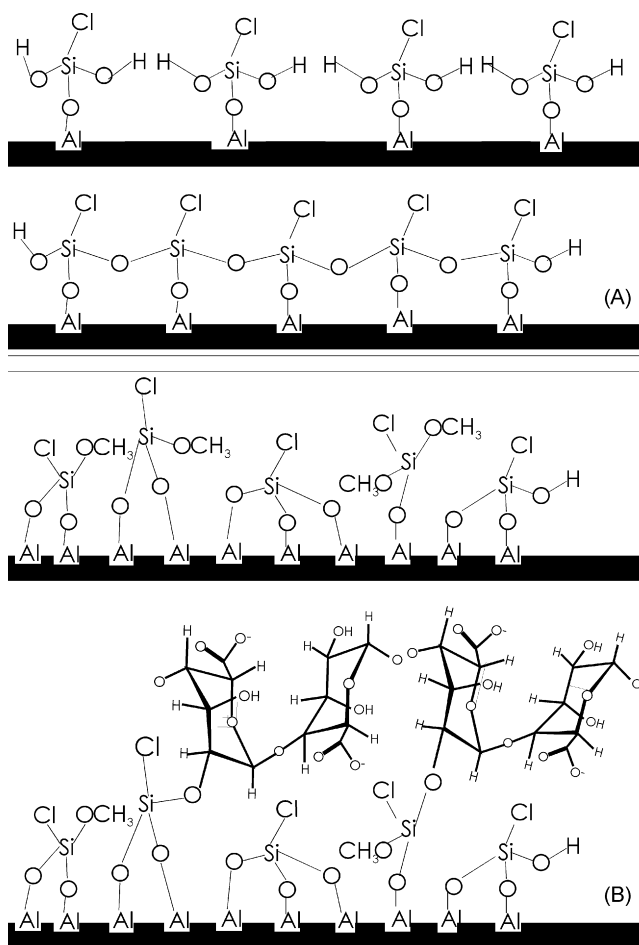


Fig. 5. (a) Polymerisation of chlorosilane bonded on non-activated g-alumina surface and (b) chlorosilane bonded on activated alumina/reaction with alginate.

either the alkoxy or diol groups in the reagent and strongly depends on the acidity of the solution. As already mentioned, it is impossible to bond simultaneously all three reactive silanols of the reagent onto the surface especially in the case when the surface is moderately activated. The unreacted reagent silanols can either remain free or participate in polymeric reaction. The vicinal diols arising from opening of the oxirane ring of GPTMS can also react with Al–OH on the alumina surface to form ester bonds. The defined by the elemental analysis C content of 0.12% in the GPTMS silanised sample Al/5/s/C9/HC (Table 1), is much lower than the one predicted out of the population of surface hydroxyls for the untreated alumina Al/5 (0.29%). This is a direct indication that the occurrence of oxirane ring opening due to the conditions developed during silanisation and the resulting surface coverage conforms to the one presented in Fig. 6a. The silane molecules were anchored on the surface through both their methoxy and diol groups forming Al–O–Si bonds and glycol ether bonds Al–O–C respectively and this had as a direct result their moderate accommodation on the alumina surface. The opening of the oxirane ring, especially when working with organic solvents, is frequently referred in the literature [9,11,17].

In this context, a different procedure was implemented by involving aquatic solutions of GPTMS with pH of 7 and pH of 8.5, the second tuned with a NaOH 1N solution. The primary objective was to avoid the opening of the oxirane ring during the surface-bonding phase. The results of the direct surface titration to the crystal violet end-point [14] for the oxirane groups and of the periodate oxidation method [9] for the surface diols are presented in Table 3 along with

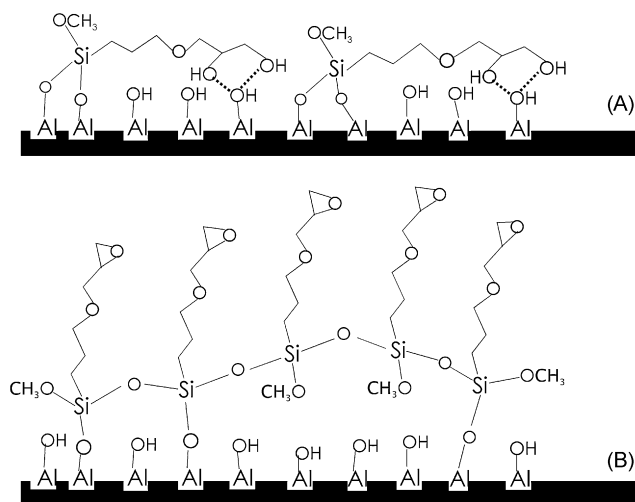


Fig. 6. (a) GPTMS grafted through methoxy and diol groups and (b) polymerisation of the GPTMS molecules through their methoxy groups.

the carbon content defined by elemental analysis and the calculated out of that oxirane group content.

The titration results showed that 80–90% of the grafted GPTMS amount retained the oxirane ring intact during the aforementioned silanisation procedure.

However, the results of elemental analysis gave a carbon content of 0.32% and 0.9% for the Al/5/s/C9/OH7/CF and Al/5/s/C9/OH8.5/CF samples respectively, which were far below the predicted value of 1.83% (see Table 1). Due to the high percentage of oxirane ring groups, a silanisation procedure like the one presented in Fig. 6a is not possible and a GPTMS grafting configuration like the one of Fig. 6b seems more probable. In this case, the high pH of the aquatic solution favors the fast hydrolysis and polymerisation of the GPTMS molecules through their methoxy groups. Thus, bulkier polymerised silanes reach the alumina surface and are anchored in an accommodation similar to the one presented in Fig. 6b. Although the surface hydroxyls are not completely consumed due to steric effects between the bulky silanes, there exists an excess of oxirane groups available for further opening (alginic solution pH = 4.5) and binding with the alginates as was also confirmed by means of the carbon content of 0.56% detected through the elemental analysis of the sample Al/5/s/C9/OH7/alg/CF (Table 1).

Consequently, as will be shown in the following sections, the water silanised sample exhibited the best metal retention capacity due to enhanced alginate loading through the reaction with the vicinal diols.

### 3.3. Performance results

#### 3.3.1. Untreated silica and alumina membranes

The Cd<sup>2+</sup> retention efficiency  $R\%$  of the untreated Al/10, Al/5, Si/1 membranes as a function of the total water volume collected from the permeate side is presented in the following Fig. 7. The retention efficiency  $R\%$  was calculated by means of Eq. (1) in case of the CF and Eq. (2) in case of the FT mode:

$$R (\%) = 100 \times \left( 1 - \frac{C_{\text{perm}}}{C_{\text{ret}}} \right) \quad (1)$$

$$R (\%) = 100 \times \left( 1 - \frac{C_{\text{perm}}}{C_{\text{feed}}} \right) \quad (2)$$

where  $C_{\text{perm}}$ ,  $C_{\text{ret}}$  and  $C_{\text{feed}}$  are the Cd<sup>2+</sup> concentrations (ppm) in the permeate, retentate and feed side of the membrane defined by AAS spectroscopy.

**Table 3**  
Experimentally determined epoxide content.

	C content from elemental (%)	Oxirane concentration from elemental ( $\mu\text{mol/g}$ )	Epoxide titration ( $\mu\text{mol/g}$ )	vis-OH titration ( $\mu\text{mol/g}$ )	Epoxide loss (%)
Al/5/s/C9/OH7/CF	0.32	33.3	26.35	12.6	21
Al/5/s/C9/OH8.5/CF	0.9	93.7	87.9	3.1	6.2

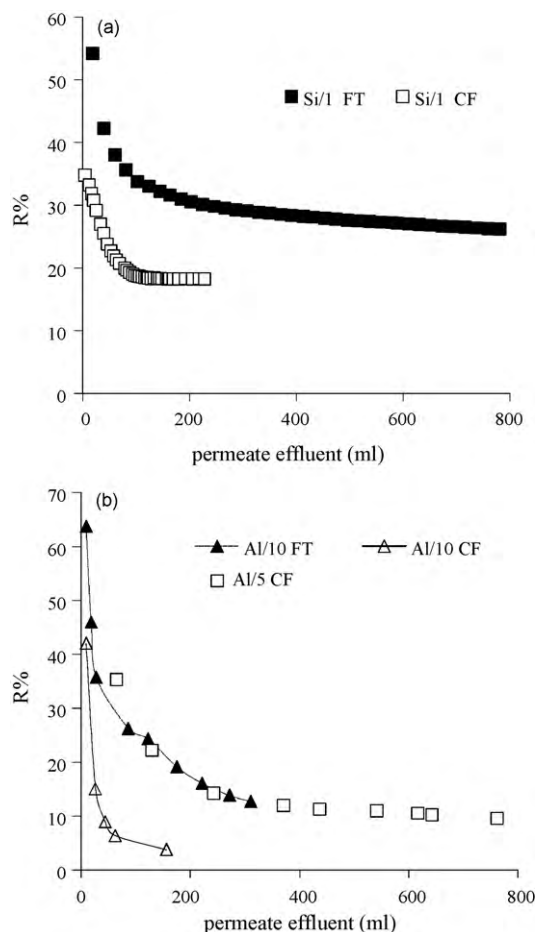


**Fig. 7.** (a) Comparison of the FT & CF experimental retention efficiency of the NF silica membrane. (b) Comparison between the FT & CF experimental retention efficiency of UF alumina of different layer pore size.

As it has been demonstrated in the examination of both materials, the flow-through method leads to an overestimation of the calculated retention efficiency that can be explained in terms of electrostatic and dielectric [18,19] exclusion phenomena occurring in charged NF/UF membranes. This means that some of the  $\text{Cd}^{2+}$  cations are binded on the negatively charged groups of the solid surface and some are prohibited to enter the pore structure due to repulsion effects. As a result, a continuous enhancement of the solute concentration in the retentate side occurs, which, however, cannot be practically defined in the FT set-up where the retention efficiency  $R\%$  is calculated over the nominal feed concentration. In order to have a more clear view on what happens in each type of the membranes examined, the main factors affecting the membrane retention efficiency, such as the charging properties and its variation among the solute concentration, the kind of solute, the pH and the pore size, have to be considered. However, it should be noted that certain aspects concerning the effect of the supporting intermediate g-alumina layer on the performance of the silica membrane, although often discussed in literature for bi-layered materials [20], are not taken into account in the current study. This

is because in the current study the pore size of the intermediate layer (200 nm) was large enough so as to have significant contribution on the metal retention efficiency.

For a PSZ of 3, like in the case of silica [21] and a solution pH of 4.8, the surface concentration of the deprotonated Si–OH ionisable groups is much higher than this of the protonated. As a result, the net surface charge is negative and cadmium ions can be adsorbed on the Si–O<sup>−</sup> groups leading to the formation of positively charged complexes (Si–(OCd)<sup>1+</sup>).

On the other hand, the adsorption of  $\text{SO}_4^{2-}$  on to the Si–(OH)<sub>2</sub><sup>+</sup> groups can lead to negatively charged complexes of the type Si–(OH<sub>2</sub>SO<sub>4</sub>)<sup>−</sup>. Due to the lower concentration of the Si–(OH<sub>2</sub>SO<sub>4</sub>)<sup>−</sup> complexes ( $\text{SO}_4^{2-}$  are initially repelled from the pores because of the negative surface charge) and the large concentration of the solute (100 ppm, 0.88 mol/m<sup>3</sup>) an overcompensation of the starting negative surface charge occurs that finally leads to a positively charged silica surface [22]. Thereinafter  $\text{Cd}^{2+}$  ions are electrostatically repulsed (electrostatic exclusion) and moreover, due to the low pH (4.8) the proton concentration in the system increases and thus, influences the retention of the other ions. In both the pore and the effluent, the slow  $\text{Cd}^{2+}$  cations (low mobility) are replaced by the much faster protons. Finally, the small pore size of the NF membrane reduces the permittivity of the water in the pores, which is lower than the bulk permittivity, thus creating an additional energy barrier for the  $\text{Cd}^{2+}$  ions to enter the pore (dielectric exclusion).

Additional evidence to the above-described mechanism for the silica membrane is presented in Fig. 8a where the amount of  $\text{Cd}^{2+}$  retained on the membrane is calculated from the mass balance between the feed, permeate and retentate membrane sides, as a function of the total  $\text{Cd}^{2+}$  feed. The corresponding curves were obtained by means of Eq. (3), applied for both the CF and FT experiments:

$$10^3 A (\text{mg}) = \int_0^t C_{\text{feed}} F t \, dt - \sum_{i=0}^t (V_{\text{per}})_i (C_{\text{per}})_i - \sum_{i=0}^t (V_{\text{ret}})_i (C_{\text{ret}})_i \quad (3)$$

where  $F$  (ml/min) is the constant flow rate of the HPLC pump,  $t$  (min) the time elapsed from the start of the experiment,  $(V_{\text{per}})_i$  and  $(V_{\text{ret}})_i$  (ml) the liquid volume collected from the permeate and retentate side at the specific time interval and  $(C_{\text{per}})_i$  and  $(C_{\text{ret}})_i$  (ppm) the corresponding  $\text{Cd}^{2+}$  concentrations. As it is clearly demonstrated (Fig. 8a), at the early stages of the process the calculated amount of retained cadmium in the FT and CF modes is almost identical, whereas the  $\text{Cd}^{2+}$  adsorption gradually alters the surface charge through the formation of Si–(OCd)<sup>1+</sup> complexes and the two curves start to deviate. In this manner, at higher flooding volumes the  $\text{Cd}^{2+}$  retention curve deviates positively in the FT mode since the amount of repulsed cadmium that has not reached the membrane pores is also included in the calculations.

It should be noted that although the pressure difference was much higher in the FT experiment (Table 2), in both cases the experiments were performed within the limiting retention area (above 4 MPa), where water transport is convective and consequently not favored over solute transport due to pressure difference increments [23].

Concerning the g-alumina membranes, the beneficial effect of the pore size reduction to the retention efficiency (Fig. 8b curves

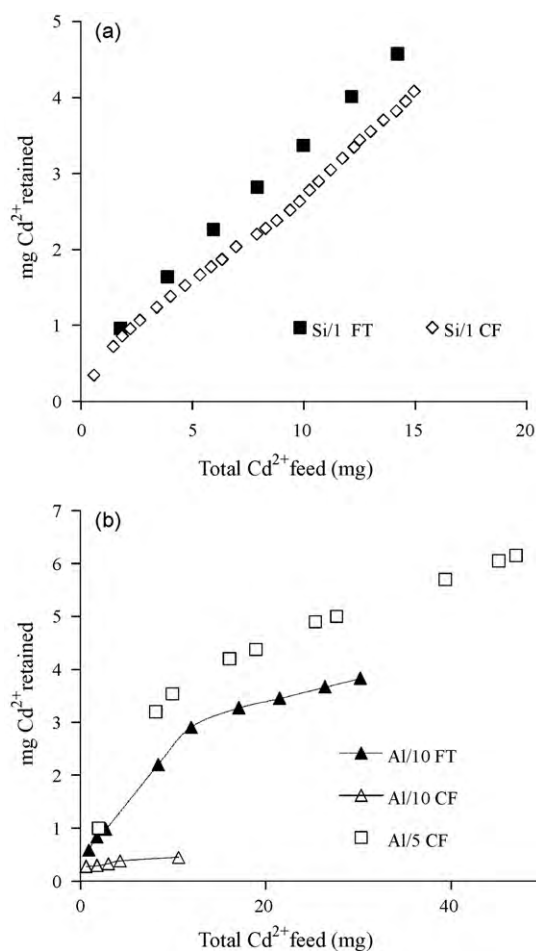


**Fig. 8.** (a) Evolution of the Cd<sup>2+</sup> amount retained on the NF silica membrane during the FT & CF experimental modes. (b) Comparison between the FT & CF experimental Cd<sup>2+</sup> amount retained on the UF alumina membranes of different layer pore size.

Al/10 CF and Al/5 CF) could clearly be observed, as well as an enhancement of the difference in the metal retention efficiency between the CF and FT modes when compared with the respective experimental modes of the silica membranes. This was an indication that the dominant retention mechanism in the examined g-alumina membranes is charge exclusion, something which was expected since at pH = 4.8 the g-alumina surface with a PCZ of 8.5 [24] is positively charged and metal cations are repelled from entering the pores. However the interpretation of the cross-flow results and especially for the 5 nm membrane concluded into a significant amount of adsorbed Cd<sup>2+</sup> that was about 3.5 mg for 10 mg of total Cd<sup>2+</sup> feed (Fig. 8b). This was unexpectedly higher than the respective amount for the negatively charged silica membrane that was 2.8 mg. It has been shown in several concluded studies that there is a specific interaction of the g-alumina surface with divalent cations [24,25], which are adsorbed even at low pH values far below the PCZ point. The different population and activity of the surface hydroxyls between the two materials (aluminol sites are known to be more reactive than silanol groups [26]) may be also a reasonable explanation but further studies were not conducted with respect to the investigation of this issue.

Finally, the g-alumina membrane with the larger pores (10 nm), exhibited a minor metal retention efficiency that was below 0.5 mg. This finding emphasizes the significant effect of the pore size on not only the overall retention efficiency, but also on the capacity of the material to bind the Cd<sup>2+</sup> ions forming surface complexes. In addition to this, strong supporting evidence is provided to the

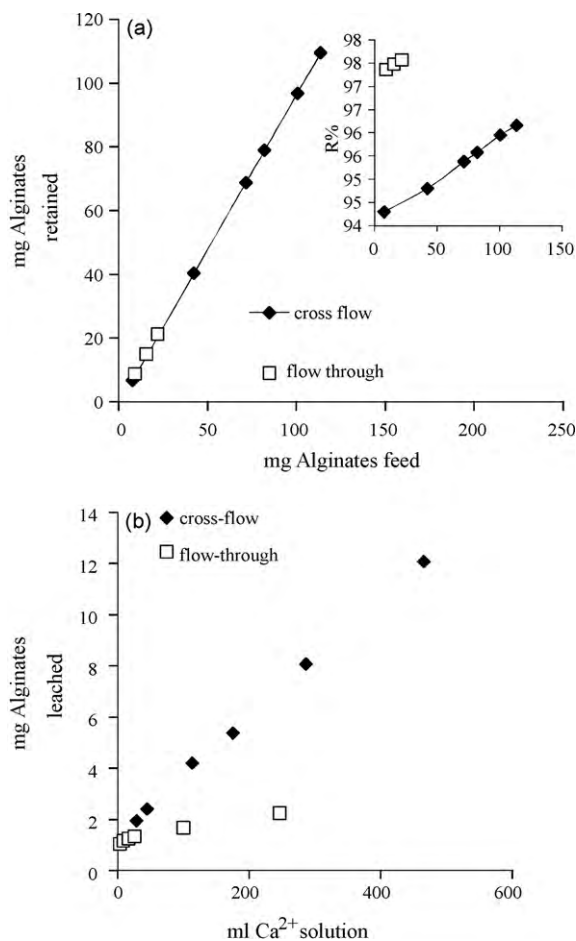


**Fig. 9.** (a) Amount of alginates retained on the UF alumina membrane during the FT and CF experimental alginate filtering modes. (b) Amount of alginates leached out from the UF alumina membrane during the FT and CF modes of cross-linking with the Ca<sup>2+</sup> solution.

previous statement that the contribution of the intermediate g-alumina supports, with even larger pore size, is negligible.

### 3.3.2. Filtration-derived alumina membranes

The characteristic curves of alginates filtration/cross-linking on the 5 nm g-alumina ultrafiltration membranes are presented in Fig. 9. The amount of retained alginates during filtration was defined with an equation similar to Eq. (3). The respective concentrations of the polymer in the different effluent streams of the reactor were determined by TOC analysis. The detected carbon mass was converted to the net mass of the alginic acid polymer by multiplying with the factor 2.43, as defined from the stoichiometry of the alginic acid monomer ((C<sub>6</sub>H<sub>8</sub>O<sub>6</sub>)<sub>n</sub>).

It is of significant interest the fact that there was not any deviation between the retention curves obtained from the CF and FT techniques (Fig. 9a). To this end, it can be stated that electrostatic exclusion phenomena are negligible and that the dominant mechanism of alginates entrapment was molecular sieving. The slight deviation from the expected 100% retention efficiency (inset Fig. 9a) observed in both modes can be attributed to the fact that the applied polymer exhibited a wide MW distribution and some of the polymeric chains with low MW could penetrate the 5 nm pores.

The FT technique proceeded by filtering the solution in the direction from the support to the inner separating layer of the membrane whereas the opposite direction was followed in the CF mode. Thus, in the former case, alginates were continuously entrapped into the larger pores of the successive support layers rather than repulsed,

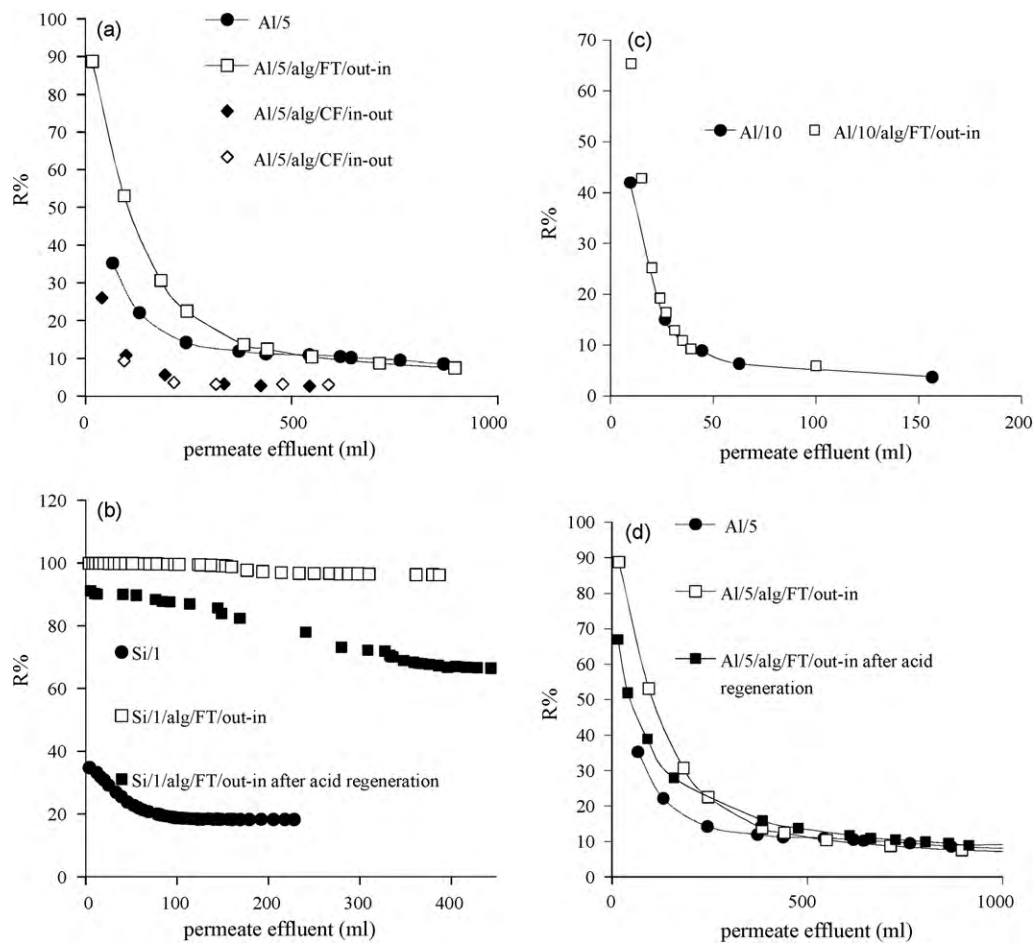


**Fig. 10.** (a) Retention efficiencies of the physically modified and pristine UF 5 nm alumina membranes. (b) Comparison of the pristine and physically modified NF 1 nm silica concerning the retention efficiency. (c) Convergence of the pristine and modified UF 10 nm alumina concerning the retention efficiency. (d) Effect of the acid regeneration on the retention efficiency of the physically modified UF 5 nm alumina membrane.

while in the later case, alginates were accumulated on the top of the membrane ultrafiltration layer forming a quite extended deposit.

The stability of the alginates that were either entrapped into the support pores or deposited on the separating layer was evaluated by determining their content into both the calcium chloride solution effluent that was subsequently applied as a cross-linking agent and the effluents gathered during the metal retention/regeneration experiments.

The curves depicted in Fig. 9b represent the amount of the removed alginates as a function of the volume of the  $\text{CaCl}_2$  solution collected at the permeate side. It may be deduced that in both cases, about 10% of the retained alginates was leached out of the membrane. However in the FT mode (Fig. 9b) the curve has reached a plateau and the total amount of alginates leached out from the permeate side corresponds to those with a low molecular weight ( $\text{MW} < 7.5 \text{ kDa}$ ) that were not cross-linked and could penetrate through the pores of the ultrafiltration layer. However and in contradiction, in the CF technique a linear relationship holds for a  $\text{CaCl}_2$  solution volume up to 600 ml. In this case, alginates eluted in the permeate side of the membrane also corresponded to the ones with a low molecular weight, while those obtained in the retentate side were leached out from the thick film that was formed on the top of the ultrafiltration layer during deposition. The leaching curve had not reached a plateau and this explains the moderate  $\text{Cd}^{2+}$  retention performance subsequently defined by means of the two cross-flow derived membranes compared to the pristine

g-alumina (Fig. 10a). Thereby, alginates with bound  $\text{Cd}^{2+}$  cations eluted in the aliquots gathered from the retentate side of the reactor, giving rise to enhanced  $\text{Cd}^{2+}$  concentrations. Additionally the presence of alginates on the top-separating layer of the membrane masked considerably the positive surface charge of g-alumina, thus eliminating the electrostatic repulsion effects. On the other hand, the FT derived membrane presented significantly improved retention efficiency that converged to that of the pristine membrane after a total permeate effluent volume of 500 ml (Fig. 10a).

Based on this concept, it can be claimed that this membrane exhibits a hybrid metal retention mechanism that comprises from the charge exclusion effect of the intact g-alumina layer and the high binding capacity of the carboxylic groups of the alginates. When all the carboxylic groups are consumed, charge exclusion caused by the separation layer becomes the dominant metal retention mechanism. In order to derive the net metal adsorption capacity of the filtered/cross-linked alginates, the metal retention curve of the pristine Al/5 membrane was subtracted from this of the Al/5/alg/FT membrane (Fig. 11a) and up to a total  $\text{Cd}^{2+}$  feed of 45 mg, that corresponds to the point where the performance curves come into convergence (Fig. 10a). The defined  $\text{Cd}^{2+}$  amounts were normalized over the net mass of the deposited alginates, which was 19 mg, as calculated from the mass balance curves obtained during the procedures of alginates filtration and subsequent cross-linking (Fig. 9a and b). The derived  $\text{Cd}^{2+}$  sorption isotherm, presented in Fig. 11b, can be compared with the relevant isotherm obtained in a previous study at the same conditions of pH and tempera-

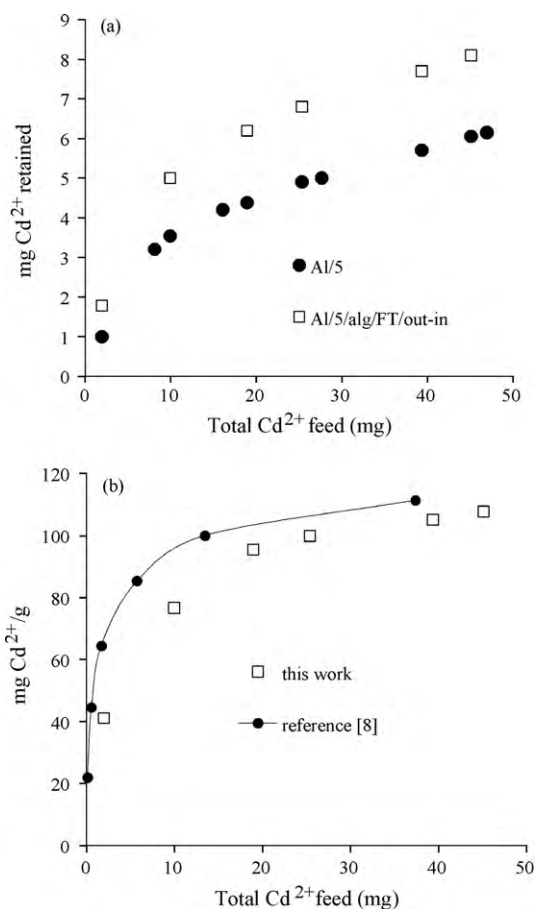


**Fig. 11.** (a) Cd<sup>2+</sup> adsorption isotherms for the pristine and physically modified UF 5 nm alumina membranes. (b) Comparison between this isotherm and the one referred in the literature for a sample of calcium alginate beads.

ture on a sample of calcium alginate beads prepared by a similar cross-linking procedure [8].

Although the leaching curve of alginates as a function of the CaCl<sub>2</sub> solution volume seems to have reached a plateau, (Fig. 9b), and several washings with an excess of deionised water (500 ml) succeeded the cross-linking procedure, the defined lower adsorption capacity (Fig. 11b) is an indication that a portion of the filtered alginates was still leached out of the membrane pores during the first metal retention test. This was something further confirmed by the detection of carbon in the solution gathered from the effluent streams (see Table 4), of the reactor and also by the continuous increase of the water permeability factor (Fig. 12a and b).

It is important to note that during the second metal retention test, the permeability was stable (Fig. 12 a and b) indicating that uncross-linked alginates were almost completely leached out of the pores during the first acidic regeneration procedure. In this manner, the hybrid membrane performance after the acidic treatment can be compared to this of the pristine membrane. This may provide clear evidence with respect to the efficiency of the process and the overall possible improvements achieved as a direct result of the modification procedures implemented.

Under this framework, the graphs compiled and depicted in Fig. 13 represent the evolution of the % improvement of the metal retention efficiency for the hybrid membranes. The completely different behavior between the modified ultrafiltration and modified nanofiltration membrane can be easily deducted and graphically assessed. During the first run, the hybrid ultrafiltration g-alumina membrane exhibited a continuous decrease of the % improvement factor, which is consistent with the consumption of the metal bind-

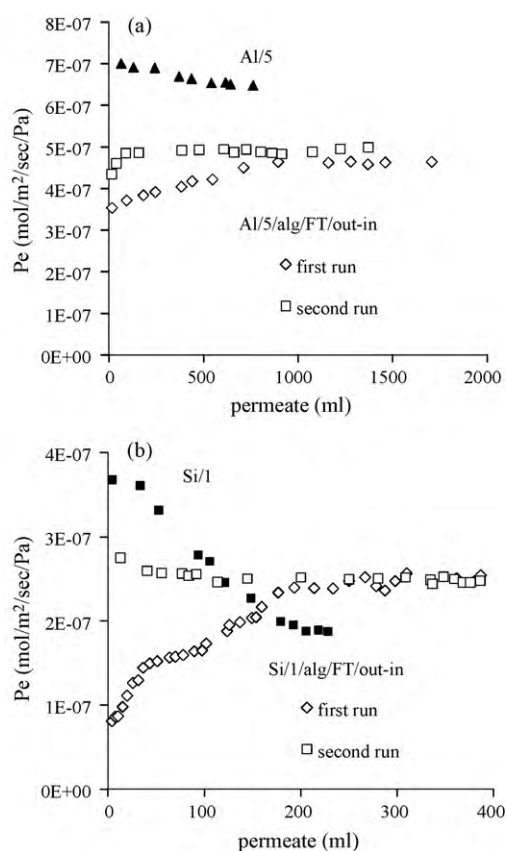


**Fig. 12.** Permeability evolution of (a) the pristine and physically modified UF 5 nm alumina membrane and (b) the pristine and physically modified NF 1 nm silica membrane.

ing carboxyl groups. From this point, the metal retention efficiency is lower than this of the untreated membrane as a result of the elution of Cd<sup>2+</sup> bearing alginates into the effluent streams of the reactor. Thereby, the curve of the second run is more characteristic for the real performance of the modified membrane (see Fig. 10b and d). The remaining stabilised alginates (2.85 mg see Table 4) resulted to a moderate improvement of the retention efficiency during the initial stages of the run, not only as a consequence of their lower amount, but also due to the fact that cross-linking consumes a large number of the Cd<sup>2+</sup> binding groups.

Interesting enough is the fact that as soon as all of the alginate carboxylic groups are consumed and charge exclusion induced by the g-alumina ultrafiltration layer becomes the dominant mechanism (steady state), the hybrid membrane preserves 8% higher metal retention efficiency compared to the untreated g-alumina membrane. The low water permeability factor observed for the hybrid membrane during the second run (Fig. 12a), which was about 70% of that of the pristine membrane, can be considered as the main cause for the preservation of this slightly higher retention efficiency. It should be noted that the low amount of alginates (2.85 mg) remained before the second metal performance test cannot justify the observed intense drop of the permeability factor if assuming that alginates were just entrapped into the larger pores of the membrane intermediate layers. As already shown, the fraction of alginates with low molecular weight can penetrate the pores of the ultrafiltration layer and it is believed that their entrapment and stabilization into the small 5 nm pores is the reason for the increase of the metal retention efficiency in the steady state.

In the case of the modified silica nanofiltration membrane, the evolution of the metal retention efficiency improvement followed the exact opposite trend. The dielectric exclusion phenomena seem

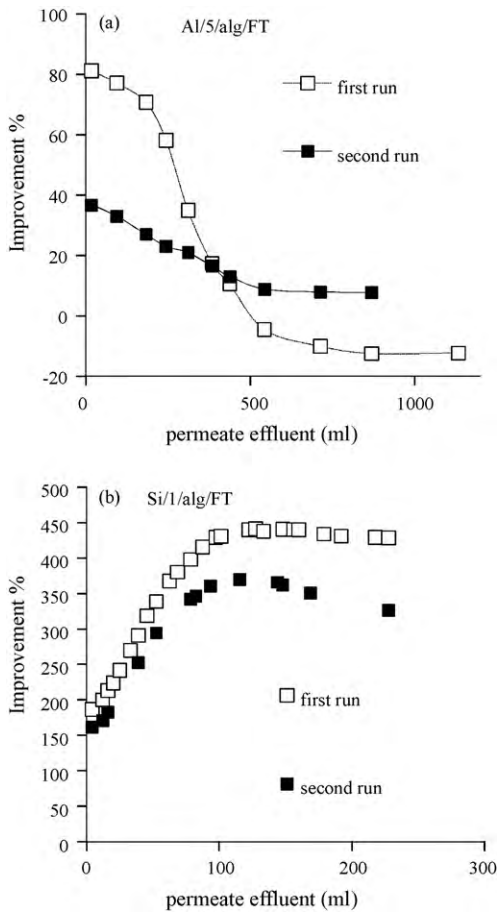


Fig. 13. Calculated retention efficiency improvement for (a) the UF 5 nm alumina membrane and (b) the NF 1 nm silica membrane.

to be the dominant retention mechanism even from the early stages of the run. The continuous increase of the improvement factor is the result of Cd<sup>2+</sup> binding on the carboxylic groups of the lower MW's alginate polymers that were stabilised in the small nanofiltration pores. Although the consumption of the -COOH binding sites should lead to a continuous decrease of the retention efficiency, in this case there is an opposite behavior due to the extremely low pore size (1 nm) of the starting material. The binding of Cd<sup>2+</sup> reduces the pore size, below 1 nm and blocks drastically the passage of the next incoming Cd<sup>2+</sup> cations.

Table 5 provides an overview of the performance improvement induced after the procedure of alginate filtration-cross-linking. This is expressed in terms of both the metal retention capacity from a stream of polluted water and the metal recovery capacity during regeneration with an acidic (HNO<sub>3</sub>) solution. The second performance runs of the unmodified membranes are intentionally omitted since the metal recovery after the first run was negligible. Consequently the metal binding capacity during the second run may be the result of mechanisms rather than adsorption ones.

3.3.3. Reaction-derived membranes

The metal retention efficiency of the reaction-derived membranes is presented in Fig. 14a and b. The efficiencies of the pristine and the filtration-derived membranes are also included. As it is clear, the chemical modification procedure resulted to hybrid materials with much better performance.

Amongst the reaction-derived membranes, the one silanised with the glycidoxysilane (GPTMS) in water (Al/5/s/C9/OH7/alg/CF) exhibited the best metal removal capacity. More specific, the

Table 4  
Stability of the physically and chemically modified UF 5 nm alumina membrane.

Run	Loading silane (mg)	Total loading silanes + alginates (mg)	Loading alginates (mg)	Amount of alginates leached away (mg)		1st acid	H <sub>2</sub> O	Amount remained before 2nd Cd <sup>2+</sup> run
				Ca <sup>2+</sup> solution	H <sub>2</sub> O			
1	2	3	4	5	6	8	9	10
Al/5/s/C9/OH7/alg/CF	257.36	199.15	88	24.98	29.19	17.52	0.015	16.41
% alginates released			21.37	0.12	46	74	74	
Al/5/alg/FT/out in						2.46	0.08	2.85
% alginates released						84	85	

**Table 5**

Overview of the performance improvement after the alginate filtration-cross-linking.

	First Cd <sup>2+</sup> run		1st acid Recovered Cd <sup>2+</sup> (mg)	Second Cd <sup>2+</sup> run		2nd acid Recovered Cd <sup>2+</sup> (mg)
	Cd <sup>2+</sup> feed (mg)/retained Cd <sup>2+</sup> (mg)	Total Cd <sup>2+</sup> feed (mg)/retained Cd <sup>2+</sup> (mg)		Cd <sup>2+</sup> feed (mg)/retained Cd <sup>2+</sup> (mg)	Total Cd <sup>2+</sup> feed (mg)/retained Cd <sup>2+</sup> (mg)	
Al/5	10/3.7	285/14.7	0.11	–	–	–
Al/5/alg/FT	10/5.1	165/13.1	7.13	10/3.9	165/11.3	8.35
Si/1	10/2.9	23/7.2	0.38	–	–	–
Si/1/alg/FT	10/8.7	11/9.3	6.3	10/8.0	24/14.7	7.2

achieved Cd<sup>2+</sup> retention factor (*R*%) was 100% for the first 100 ml of water effluent. Thereinafter, with the elution of about 1500 ml of water, the retention efficiency came into converge with this of the pristine sample (Al/5). This leads to the conclusion that the induced performance improvement arises as a consequence of the higher alginate loading, which was achieved by preventing oxirane ring opening during the silanisation procedure. Indeed, the carbon content of this membrane was 0.56%, as determined by means of elemental analysis (see Table 1). An estimated 0.32% of the measured carbon content corresponded to the carbon of the glycidoxysilane grafted on the surface (Al/5/s/C9/OH7/CF, Table 1) and the rest 0.24% to the carbon of the bonded alginates. The respective carbon content of the silanised in chloroform membrane was 0.29% (see Table 1 Al/5/s/C6/HC/alg/FT), from which 0.17% corresponded to the carbon of the chlorosilane grafted on its surface (Al/5/s/C6/HC, Table 1) and 0.12% to the carbon of the bonded alginates. In Fig. 14d, a comparative analysis of the retention factor (*R*%)

evolution of the two GPTMS silanised membranes is presented. The pragmatic effect of using water instead of an organic solvent during silanisation can be clearly deduced.

The fact that the chemically modified membranes retained a higher amount of stabilised alginates can be also verified from the results presented in Table 4. The alginate amount leached away (columns 5–9) was defined by TOC analysis of the aliquots gathered from the retentate and permeate side of the membrane. The silane and alginate loading (columns 2 and 3) were calculated from the mass balance Eq. (3), with the procedure already described in Section 3.3.1. It should be noted that for the chemically modified membrane Al/5/s/C9/OH7/alg/CF, the mass balance calculation resulted in smaller value of the total silane and alginate loading (refer to columns 2 and 3), due to leaching of the non-grafted silane during the reaction with the alginate acid. The net amount of covalently bonded alginates (column 4) was calculated by taking into account the results of elemental analysis

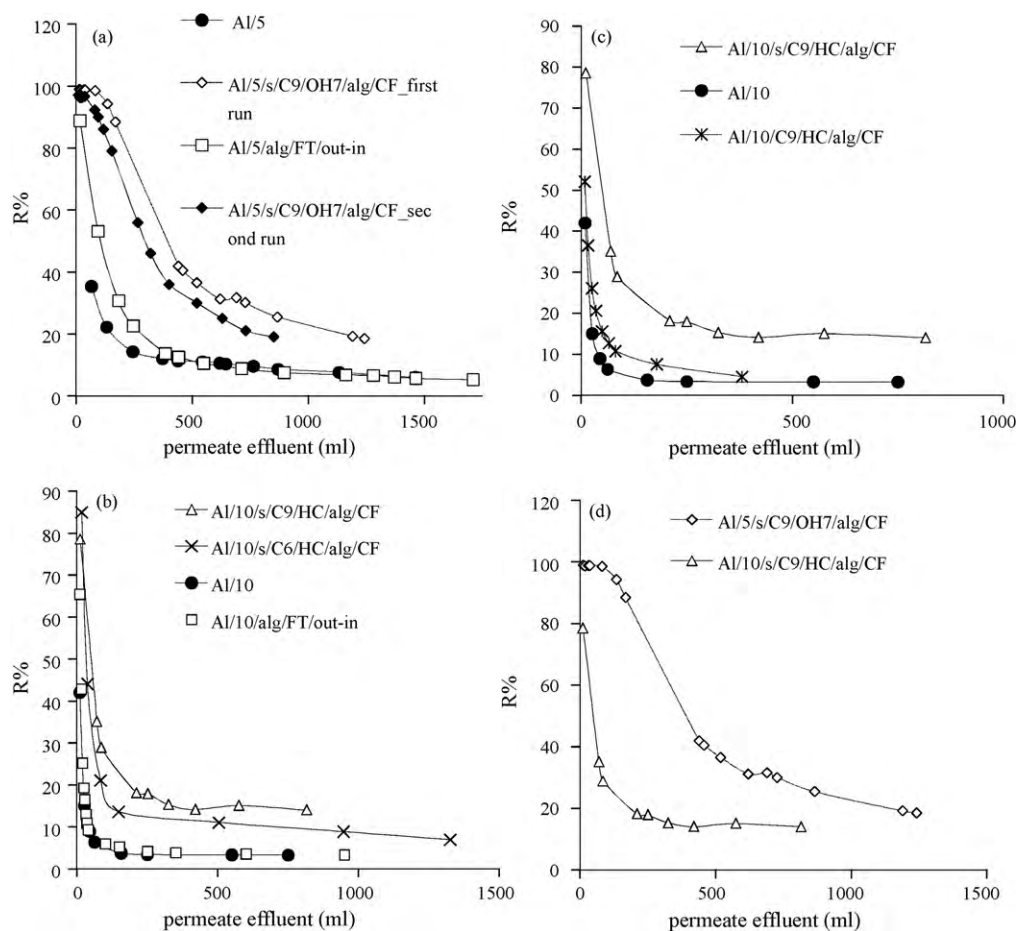


**Fig. 14.** Retention efficiencies of the chemically and physically modified samples: (a) UF 5 nm alumina and (b) UF 10 nm alumina. (c) Comparison of the pristine and the GPTMS modified (activated/non-activated surface) UF 10 nm alumina concerning the retention efficiency. (d) Retention efficiencies of the GPTMS modified UF 5 nm and 10 nm alumina membranes.

for the samples Al/5/s/C9/OH7/CF and Al/5/s/C9/OH7/alg/CF. The silane/alginate carbon ratio was equal to 1.33 (0.32/0.24). By considering the stoichiometry of the molecules the above value of the carbon ratio produces a silane/alginate mass ratio of 1.26. It can be readily deduced that before proceeding with the second Cd<sup>2+</sup> run, which, as already mentioned, is more characteristic for the improvements induced by the modification procedure, the chemically modified membrane retained a six times higher amount of alginates.

#### 4. Conclusions

The primary objective and scientific challenge of the current work was to stabilise the biopolymer on the membrane surface by means of covalent bonding without further involving a cross-linking procedure, which could neutralise a considerable portion of the polymer's metal binding groups (–COOH). The percentage of the alginate amount released in the effluent streams after the first washing process indicates their higher stability on the chemically modified membrane. The physically modified membrane released about 72% of the stabilised alginates during the first Cd<sup>2+</sup> run whereas the relevant amount for the chemically modified was 46%. The chemically modified membrane (Al/5/s/OH7/alg/CF) not only exhibited an 180% improvement of the retention efficiency over the unmodified membrane Al/5, for the first 100 ml of water effluent and of 120% up to a water effluent volume of 800 ml, but also conserved most of its ability to efficiently retain Cd<sup>2+</sup> during the second run after the acidic regeneration.

#### Acknowledgments

The authors would like to thank Dr. F. Katsaros and Dr. S. Papageorgiou for useful discussions. Financial support by the European Network of Excellence INSIDE–PORES is gratefully acknowledged.

#### References

- [1] D. Kratochvil, B. Volesky, Biosorption of Cu from ferruginous wastewater by algal biomass, *Water Res.* 32 (1998) 2760–2768.
- [2] Y.H. Gin, K.Y. Tang, M.A. Aziz, Derivation and application of a new model for heavy metal biosorption by algae, *Water Res.* 36 (2002) 1313–1323.
- [3] T. Panayotova, M. Dimova-Todorova, I. Dobrevsky, Purification and reuse of heavy metals containing wastewaters from electroplating plants, *Desalination* 206 (2007) 135–140.
- [4] M.J. Gonzalez-Munoz, M.A. Rodriguez, S.A. Luque, J.R. Alvarez, Recovery of heavy metals from metal industry waste waters by chemical precipitation and nanofiltration, *Desalination* 200 (2006) 742–744.
- [5] M. Muthukrishnan, B.K. Guha, Heavy metal separation by using surface modified nanofiltration membrane, *Desalination* 200 (2006) 351–353.
- [6] M.E. Argun, S. Dursun, C. Ozdemir, M. Karatas, Heavy metal adsorption by modified oak sawdust: thermodynamics and kinetics, *J. Hazard. Mater.* 141 (2007) 77–85.
- [7] C.P. Athanasekou, S.K. Papageorgiou, V. Kaselouri, F.K. Katsaros, N.K. Kakizis, A.A. Sapalidis, N.K. Kanellopoulos, Development of hybrid alginate/ceramic membranes for Cd<sup>2+</sup> removal, *Micropor. Mesopor. Mater.* 120 (2009) 154–164.
- [8] S.K. Papageorgiou, E.P. Kouvelos, F.K. Katsaros, Calcium alginate beads from *Laminaria digitata* for the removal of Cu<sup>2+</sup> and Cd<sup>2+</sup> from dilute aqueous metal solutions, *Desalination* 224 (2008) 293–306.
- [9] B. Porsch, Epoxy- and diol-modified silica: optimization of surface-bonding reaction, *J. Chromatogr. A* 653 (1993) 1–7.
- [10] H. Engelhardt, Chemically bonded stationary phases for aqueous high-performance exclusion chromatography, *J. Chromatogr.* 142 (1977) 311–320.
- [11] Y. Shen, Silica surface interactions of diol-bonded phases in packed capillary column supercritical fluid chromatography, *J. Microcolumn Sep.* 8 (1996) 413–420.
- [12] K. Ernst-Cabrera, M. Wilchek, Silica containing primary hydroxyl groups for high-performance affinity chromatography, *Anal. Biochem.* 159 (1986) 267–272.
- [13] X. Shao, Capillary electrophoresis using diol-bonded fused-silica capillaries, *J. Chromatogr. A* 830 (1999) 415–422.
- [14] R.R. Jay, Direct titration of epoxy compounds and aziridines, *Anal. Chem.* 36 (1964) 667–668.
- [15] M.F.L. Johnson, Surface area stability of aluminas, *J. Catal.* 123 (1990) 245–259.
- [16] H. Landmesser, H. Kosslick, U. Kürschner, R. Fricke, Acidity of substituted mesoporous molecular sieve MCM-48, *J. Chem. Soc., Faraday Trans.* 94 (1998) 971–977.
- [17] N.D. Cheronis, T.S. Ma, *Organic Functional Group Analysis by Micro and Semi-micro Methods*, Wiley, New York, 1964.
- [18] J.R. Bontha, P.N. Pintauro, Water orientation and ion solvation effects during multicomponent salt partitioning in a nafion cation exchange membrane, *Chem. Eng. Sci.* 49 (1994) 3835–3851.
- [19] E. Yaroshchuk, Dielectric exclusion of ions from membranes, *Adv. Colloid Interface Sci.* 85 (2000) 193–230.
- [20] W.B. Samuel de Lint, T. Zivkovic, N.E. Benes, H.J.M. Bouwmeester, D.H.A. Blank, Electrolyte retention of supported bi-layered nanofiltration membranes, *J. Membr. Sci.* 277 (2006) 18–27.
- [21] J.M. Skluzacek, M.I. Tejedor, M.A. Anderson, An iron-modified silica nanofiltration membrane: effect of solution composition on salt rejection, *Micropor. Mesopor. Mater.* 94 (2006) 288–294.
- [22] R.J. Hunter, *Introduction to Modern Colloid Science*, Oxford University Press, Oxford, 1993.
- [23] Y. Yang, P.N. Pintauro, Multicomponent space-charge transport model for ion-exchange membranes, *AIChE J.* 46 (2000) 1177–1190.
- [24] T.K. Sen, M.V. Sarzali, Removal of cadmium metal ion (Cd<sup>2+</sup>) from its aqueous solution by aluminium oxide (Al<sub>2</sub>O<sub>3</sub>): a kinetic and equilibrium study, *Chem. Eng. J.* 142 (2008) 256–262.
- [25] J. Lyklema, *Fundamentals of Interface and Colloid Science*, vol. 2, Academic Press, London, 1995.
- [26] F. Barbier, G. Duc, M. Petit-Ramel, Adsorption of lead and cadmium ions from aqueous solution to the montmorillonite/water interface, *Colloids Surf. A* 166 (2000) 153–159.